

Supplementary Materials

Efficient synthesis of plate-like crystalline hydrated tungsten trioxide thin films with highly improved electrochromic performance

Zhihui Jiao,^a Xiu Wang,^b Jinmin Wang,^a Lin Ke,^c Hilmi Volkan Demir^{d,e} Tien Wei Koh,^a and Xiao Wei Sun^{*a,f}

^a School of Electrical and Electronic Engineering, Nanyang Technological University, Nanyang Avenue, Singapore 639798, Singapore. Fax: +65-67933318; Tel: +65-67905369; E-mail: exwsun@ntu.edu.sg, jiao0013@e.ntu.edu.sg

^b School of Materials Science and Engineering, Nanyang Technological University, Nanyang Avenue, Singapore 639798, Singapore

^c Institute of Material Research and Engineering, A*STAR (Agency for Science, Technology and Research), Research Link, Singapore 117602, Singapore

^d Department of Electrical and Electronics Engineering, Department of Physics, UNAM--Institute of Materials Science and Nanotechnology, Bilkent University, Bilkent, Ankara 06800, Turkey

^e School of Electrical and Electronic Engineering, School of Physical and Mathematical Sciences, Nanyang Technological University Nanyang Avenue, Singapore 639798, Singapore

^f Department of Applied Physics, College of Science, and Tianjin Key Laboratory of Low-Dimensional Functional Material Physics and Fabrication Technology, Tianjin University, Tianjin 300072, China

*To whom correspondence should be addressed. Email: exwsun@ntu.edu.sg

Experimental Section

Preparation of Crystal Seeds Layers. Typically, 1.5 mL HCl solution was added into 15 mL 0.03 g/L $\text{Na}_2\text{WO}_4 \cdot 2\text{H}_2\text{O}$ solution. The formed yellowish precipitate was washed using de-ionized water in ice bath for several times and finally 50 mL mixture was obtained. Finally a WO_3 seed sol was obtained after 2 mL H_2O_2 was added into the heated mixture under intense stirring. The sol was then spin coated onto pre-cleaned FTO glasses and the seed coating substrates were heated for application.

Preparation of Precursor and Hydrothermal Treatment. $\text{Na}_2\text{WO}_4 \cdot 2\text{H}_2\text{O}$ (1g) was dissolved into 15 mL of de-ionized water and then HCl (7 mL) was added into the solution. A 100 mL mixture was finally obtained after the formed precipitate was washed using de-ionized water for many times. Under intensively stirring, H_2O_2 (3 mL) was added into the above heated suspension and a transparent solution was obtained. The solution was diluted to half concentration by de-ionized water and Na_2SO_4 (5×10^{-4} g/L) was added as the capping agent. A solution without adding Na_2SO_4 was prepared for comparison. The as-prepared solutions were transferred into autoclaves and then the WO_3 seed coating substrates were put into autoclaves. The hydrothermal reactions were kept at 180°C for 2 h. The as-grown films were washed by de-ionized water and dried in atmosphere.

Characterization. The composition of as-prepared products were characterized by a Bruker D8 X-ray powder diffraction (XRD, Siemens), using $\text{Cu K}\alpha 1$ ($\lambda = 0.15406$ nm) radiation. The phase structures were characterized by Raman spectroscopy (Renishaw inVia). X-ray photoelectron spectroscopy (XPS) data were obtained on a Kratos AXIS spectrometer with monochromatic $\text{Al-K}\alpha$ (1486.71 eV) X-ray radiation. Morphologies of the as-prepared thin films were observed by field-emission scanning electron microscopy (FESEM, JSM-6340).

High-resolution transmission electron microscope (HRTEM) images were obtained by a JEM-2010 microscope with an accelerating voltage of 200 kV. Cyclic voltammetry and chronoamperometry datas of the films were measured by a three-electrode system (VersaSTAT 3F Potentiostat/Galvanostat) with 0.5 M H₂SO₄ as the electrolyte, Pt as the counter electrode and Ag/AgCl/1M KCl as the reference electrode. The transmittance spectra were measured by a UV-Vis spectrophotometer (JESCO V670).

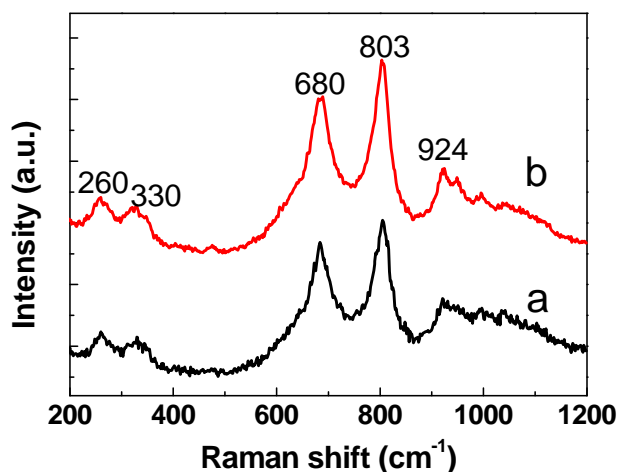


Figure S1. Raman spectra of the films. a: without Na₂SO₄. b: with Na₂SO₄.

Fig. S1 displays a Raman spectrum of the 3WO₃·H₂O films. The bands at 680 and 807 cm⁻¹ arise from the O-W-O stretching vibrations of the bridging oxygen atoms, the band at 260 cm⁻¹ belongs to W-O-W bending mode and the bands at 330 cm⁻¹ and 924 cm⁻¹ can be assigned to the stretching of W-OH₂ and W=O, respectively.^{1,2}

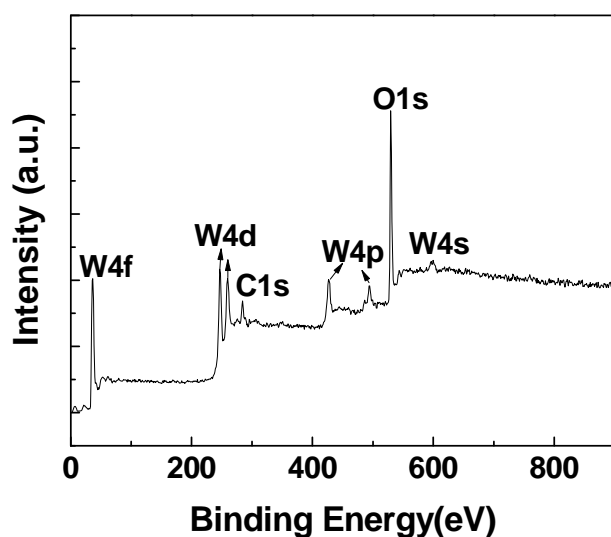


Figure S2. Wide scanning XPS spectra of the as-fabricated nanoplate films.

Fig. S2 shows the wide scanning XPS spectra of the nanoplate films. The binding energies of the sample were corrected using a value of 284.6 eV for the C 1s peak of carbon. All the peaks appeared in the spectra can be well indexed to be W and O elements. There is no contaminated element except C in the film. And it is well known that such adventitious carbon layer is usually formed for the samples exposed in the air. The above result implies the high purity of the as-grown nanoplate films.

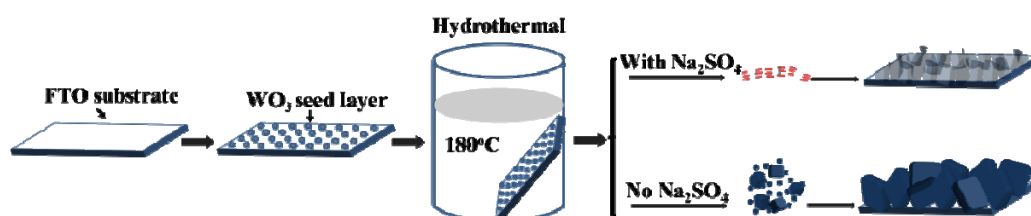
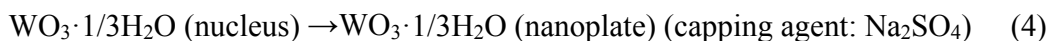
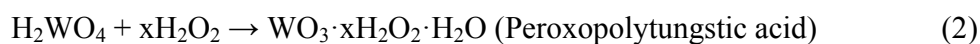
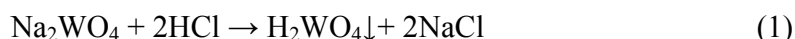


Figure S3. A schematic illustration of the formation process for $3\text{WO}_3 \cdot \text{H}_2\text{O}$ films grown with and without Na_2SO_4 .

The precipitation of WO_3 from the WO_4^{2-} containing solution and the growth mechanism of the plate-like nanostructured film can be explained according to the following well known reactions:



H_2WO_4 precipitate was formed after addition of HCl solution. Then it was dissolved by adding hydrogen peroxide (H_2O_2) and peroxopolytungstic acid (PTA) was obtained. A layer of $\text{WO}_3 \cdot 1/3\text{H}_2\text{O}$ crystal nucleus was formed from the decomposition temperature of PTA at high temperature, and the seed-coating substrate acted as nucleation and growth sites. The plate-like nanostructures were grown eventually from the $\text{WO}_3 \cdot 1/3\text{H}_2\text{O}$ nucleus under the capping agent of Na_2SO_4 , while stacked brick-like films were obtained. Fig. S3 schematically illustrates the formation process of plate-like and stacked brick-like $3\text{WO}_3 \cdot \text{H}_2\text{O}$ films grown with and without Na_2SO_4 .

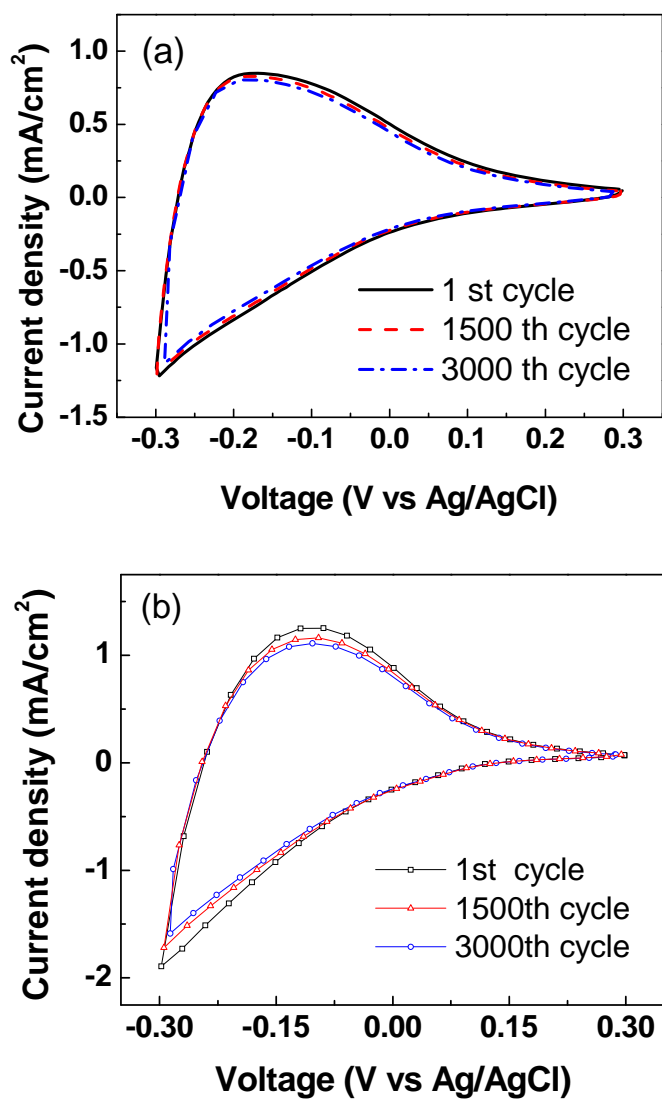


Figure S4. (a) and (b) CV curves of the films grown with and without Na₂SO₄ after the 1st, 1500th and 3000th cycles, measured in 0.5M H₂SO₄ solution at a scan rate of 0.1 V/s, respectively.

Fig. S4 (a) and (b) show the CV curves of the films grown with and without Na_2SO_4 after the 1st, 1500th and 3000th cycles, respectively. It can be seen that the nanoplate film shows good cyclic stability even in the acidic solution, since there is no significant change in the shape of the CVs, only a small reduction was observed after 3000 cycles. On the other hand, a larger current reduction was observed for the nanobrick film, indicating an inferior stability.

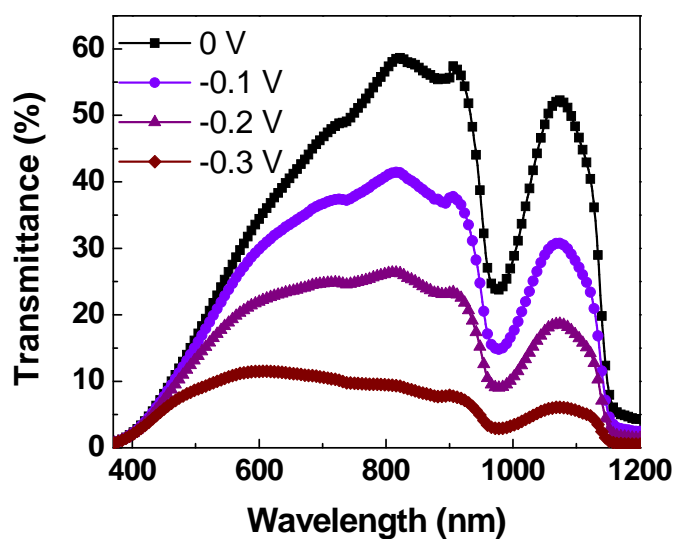


Figure S5. UV-vis transmittance spectra of the plate-like $3\text{WO}_3 \cdot \text{H}_2\text{O}$ film based EC device under 0, -0.1, -0.2 and -0.3 V, respectively.

Tunable transmittance could be obtained for the nanoplate film under -0.1, -0.2 and -0.3 V in 0.5 M H_2SO_4 solution (Fig. S5). With increased negative bias voltage, more H^+ will be inserted into the film and the color of the film will become deeper, leading to the decrease of optical transmittance above 460 nm and a blue shift of the peak transmittance from 884 to 802, 703 and 675 nm, respectively.

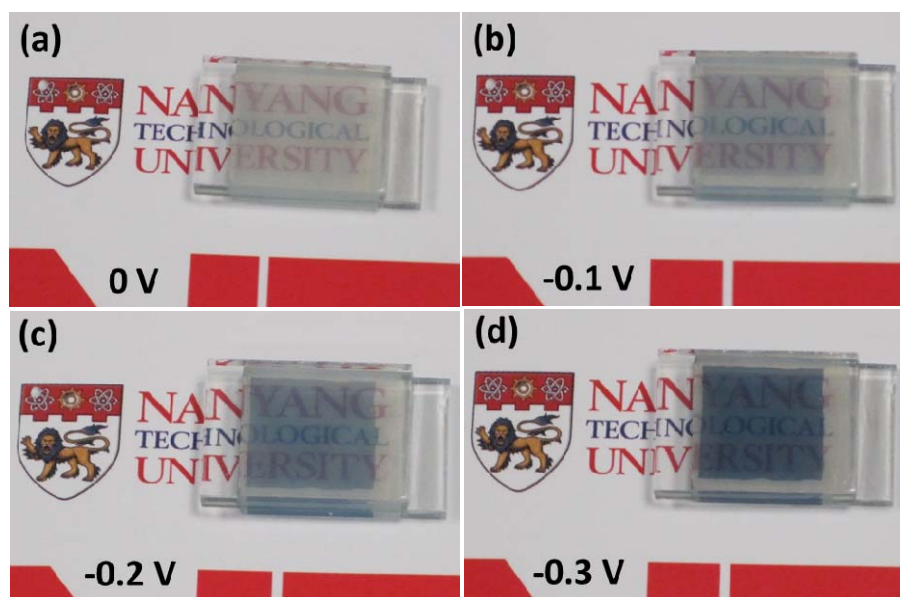


Figure S6. Photographs of the EC device made up of the nanoplate $3\text{WO}_3 \cdot \text{H}_2\text{O}$ film under 0, -0.1, -0.2 and -0.3 V, respectively.

Photographs of EC device made up with the nanoplate film grown with Na_2SO_4 under 0, -0.1, -0.2 and -0.3 V are shown in Fig. S6, depicting a high contrast between bleached and colored state which leads to the obvious transparency changes. With increased negative bias, the device shows a deeper blue color, leading to a larger optical regulation between bleached and colored state.

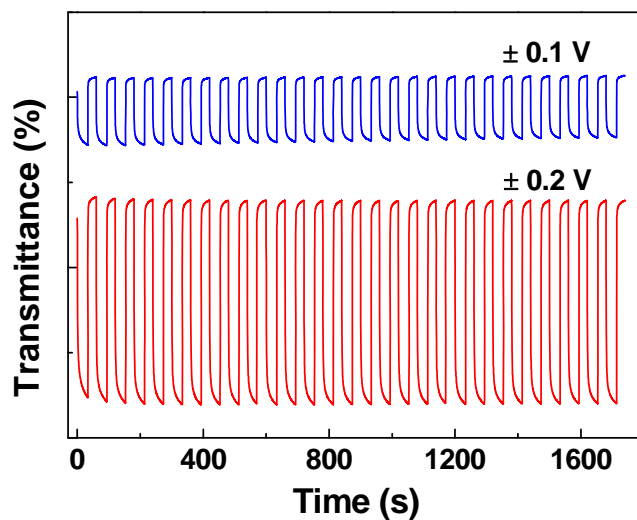


Figure S7. Switching properties of the nanoplate film under ± 0.1 V and ± 0.2 V at 632.8 nm.

Fig. S7 shows the switching response of the nanoplate film under ± 0.1 V and ± 0.2 V at 632.8 nm. When ± 0.1 V was applied, coloration time t_c and bleaching time t_b are found to be 9.2 s and 1.3 s respectively, while they are 18 s and 1 s respectively under ± 0.2 V bias. Reverse trend for coloration and bleaching speed is obtained when increasing the bias from ± 0.1 V to ± 0.3 V. And smaller optical modulations were found under these biases.

Table S1. Data for WO₃ film-based electrochromic devices found in the literature showing modulation range, the performed numbers of cyclic cycles, the switching time for coloration and bleaching and coloration efficiency.

Assembling techniques	Optical regulation	Cycles	Coloration time (t_c)	Bleaching time (t_b)	Coloration efficiency (CE: cm ² /C)
Nanoparticle film by hot-wire chemical vapor deposition [3].		3000			42 (670 nm)
Nanorod film by colloidal and spin-coating [4].	$\Delta\text{Abs (700 nm)}=0.99$	300	$t_c = 6.4 \text{ s}$	$t_b = 3.0 \text{ s}$	132 (700 nm)
Nanowire array film by hydrothermal [5].	$\Delta T (633 \text{ nm})\approx 57\%$	1000	$t_{c,90\%} = 7.6 \text{ s}$	$t_{b,90\%} = 4.2 \text{ s}$	102.8 (633 nm)
Fibrous reticulated film by spray pyrolysis [6].	$\Delta T (630 \text{ nm})\approx 10\%$		$t_c = 5.5 \text{ s}$	$t_b = 3.8 \text{ s}$	34 (630 nm)
Mesoporous film by electrodeposition [7].	$\Delta T (632.8 \text{ nm})=71\%$	1000	$t_{c,90\%} = 8.9 \text{ s}$	$t_{b,90\%} = 4.5 \text{ s}$	70 (632.8 nm)
Nanoparticle film by dip coating [8].	$\Delta T (632.8 \text{ nm})=74\%$	1500	$t_c = 111 \text{ s}$	$t_b = 55 \text{ s}$	73.6 (630 nm)
Nanoparticle film by spin-coating [8].	$\Delta T (632.8 \text{ nm}) = 62\%$	1500	$t_c = 115 \text{ s}$	$t_b = 43 \text{ s}$	51.1 (632.8 nm)
Amorphous film by oxygen sputtering [9].	$\Delta T (550 \text{ nm}) \approx 75\%$		$t_{c,84\%} = 32 \text{ s}$	$t_{b,84\%} = 8 \text{ s}$	141 (550 nm)
Nanowire film by thermal evaporation [10].	$\Delta T (700 \text{ nm}) \approx 65\%$		$t_{c,80\%} = 3.0 \text{ s}$	$t_{b,80\%} = 1.5 \text{ s}$	61.3 (700 nm)

References:

- 1 X. Zhang, X. Lu, Y. Shen, J. Han, L. Yuan, L. Gong, Z. Xu, X. Bai, M. Wei, Y. Tong, Y. Gao, J. Chen, J. Zhou and Z. L. Wang, *Chem. Commun.*, 2011, **47**, 5804.
- 2 M. F. Daniel, B. Desbat and J. C. Lassegues, *J. Solid State Chem.*, 1987, **67**, 235.
- 3 S. H. Lee, R. Deshpande, P. A. Parilla, K. M. Jones, B. To, A. H. Mahan and A. C. Dillon, *Adv. Mater.*, 2006, **18**, 763.
- 4 S.Y. Park, J.M. Lee, C. Noh, S.U. Son, *J. Mater. Chem.*, 2009, **19**, 7959.
- 5 J. Zhang, J. P. Tu, X. H. Xia, X. L. Wang and C. D. Gu, *J. Mater. Chem.*, 2011, **21**, 5492.
- 6 S.R. Bathe, P.S. Patil, *Sol. Energy Mater. Sol. Cells*, 2007, **91**, 1097.
- 7 M. Deepa, A.K. Srivastava, K.N. Sood, S.A. Agnihotry, *Nanotechnology*, 2006, **17**, 2625.
- 8 M. Deepa, T.K. Saxena, D.P. Singh, K.N. Sood, S.A. Agnihotry, *Electrochim. Acta.*, 2006, **51**, 1974.
- 9 A. Subrahmanyam, A. Karuppasamy, *Sol. Energy Mater. Sol. Cells*, 2007, **91**, 266.
- 10 C.C. Liao, F.R. Chen, J.J. Kai, *Sol. Energy Mater. Sol. Cells*, 2007, **91**, 1258.